JAAS

PAPER

View Article Online
View Journal | View Issue

Cite this: J. Anal. At. Spectrom., 2018, 33, 231

U–Pb age determination of schorlomite garnet by laser ablation inductively coupled plasma mass spectrometry†

Yue-Heng Yang,*[ab] Fu-Yuan Wu,[ab] Jin-Hui Yang,[ab] Roger H. Mitchell,[c] Zi-Fu Zhao,[d] Lie-Wen Xie,[ab] Chao Huang,[ab] Qian Ma,[abe] Ming Yang[abf] and Han Zhao[abf]

We report the first U–Pb geochronological investigation of schorlomite garnet from carbonatite and alkaline complexes and demonstrate its applicability for U–Pb age determination using laser ablation inductively coupled plasma mass spectrometry (LA-ICP-MS) due to its relatively high U and Th abundances and negligible common Pb content. The comparative matrix effects of laser ablation of zircon and schorlomite are investigated and demonstrate the necessity of a suitable matrix-matched reference material for schorlomite geochronology. Laser-induced elemental fractional and instrumental mass discrimination were externally-corrected using an in house schorlomite reference material (WS20) for U–Pb geochronology. In order to validate the effectiveness and robustness of our analytical protocol, we demonstrate the veracity of U–Pb age determination for five schorlomite samples from: the Magnet Cove complex, Arkansas (USA); the Fanshan ultrapotassic complex, Hebei (China); the Ozernaya alkaline ultramafic complex, Kola Peninsula (Russia); the Alnö alkaline–rock carbonatite complex (Sweden); and the Prairie Lake carbonatite complex, Ontario (Canada). The schorlomite U–Pb ages range from 96 Ma to 1160 Ma, and are almost identical to ages determined from other accessory minerals in these complexes and support the reliability of our analytical protocol. Schorlomite garnet U–Pb geochronology is considered to be a promising new technique for understanding the genesis of carbonatites, alkaline rocks, and related rare-metal deposits.

Received 14th September 2017
Accepted 10th January 2018

DOI: 10.1039/c7ja00315c

rsc.li/jaas

1. Introduction

Schorlomite $[Ca_3(Ti,Fe^{3+})_2(Si,Fe^{3+},Fe^{2+})_3O_{12}]$ is a species of garnet belonging to the garnet super group, containing more than one atom of titanium per formula unit (>15 wt% TiO_2).[1] Garnet has the ability to record the conditions and timing of its growth in its major, trace element and isotopic characteristics. Previously, only Sm–Nd and Lu–Hf methods have been used for garnet age determination.[2,3] Schorlomite U–Pb geochronology has a number of advantages over destructive methods of Sm–Nd or Lu–Hf isotopic analysis using isotope dilution (ID) thermal ionization mass spectrometry (TIMS) or multiple collector inductively coupled plasma mass spectrometry (MC-ICP-MS). In contrast, *in situ* methods such as LA-ICP-MS or secondary ion mass spectrometry (SIMS), do not require a co-genetic phase or whole rock measurement in order to calculate an age. Recently, Seman *et al.*[4] presented U–Pb geochronology of grossular-andradite garnet using LA-ICP-MS and developed three potential reference materials for LA-ICP-MS. However, the sample investigated has a low U content (<10 ppm) in addition to significant amounts of common Pb. Deng *et al.*[5] demonstrated U–Pb age determination by LA-ICP-MS for andradite-rich garnet in alkaline igneous rocks and skarn deposits. The consistency between the garnet and zircon U–Pb ages confirms the reliability and accuracy of garnet U–Pb geochronology using zircon (91 500) as external calibration standard.

To the best of our knowledge, there are no of definitive U–Pb geochronological studies of schorlomite or analytical protocols for U–Pb age determinations reported in the available literature regardless of the wide occurrence of schorlomite in alkaline, carbonatite, syenite, phonolite, skarn rocks, and related rare metal deposits.[6] Alkaline and carbonatitic rocks are an important

[a]State Key Laboratory of Lithospheric Evolution, Institute of Geology and Geophysics, Chinese Academy of Sciences, P. B. 9825, Beijing, 100029, P. R. China. E-mail: yangyueheng@mail.iggcas.ac.cn; Fax: +86-010-62010846; Tel: +86-010-82998599
[b]Institutions of Earth Science, Chinese Academy of Sciences, Beijing, 100029, P. R. China
[c]Department of Geology, Lakehead University, Ontario, P7B 5E1, Canada
[d]CAS Key Laboratory of Crust-Mantle Materials and Environments, School of Earth and Space Science, University of Science and Technology of China, Hefei, 230026, P. R. China
[e]State Key Laboratory of Geological Processes and Mineral Resources, School of Earth Science and Resources, China University of Geosciences, Beijing, 100083, P. R. China
[f]University of Chinese Academy of Sciences, Beijing 100049, P. R. China

† Electronic supplementary information (ESI) available. See DOI: 10.1039/c7ja00315c

petrological record of magmatic intrusion, and provide information for deciphering the geodynamic evolution of ancient continental blocks.[7,8] Direct age determination of alkaline rocks and carbonatites is typically limited to accessory minerals including: Re–Os for molybdenite; U–Pb for titanite, zircon or apatite; and or Rb–Sr and K–Ar or Ar–Ar for micas. However, schorlomite is a common primary product of crystallization and can potentially be used for U–Pb age determination.

In this study, we initially present an analytical protocol for schorlomite U–Pb geochronology using LA-ICP-MS analysis. Schorlomite U–Pb age determinations can definitively constrain the emplacement ages of alkaline and carbonatitic rocks, which might not be amenable to conventional U–Pb zircon geochronology. The relative matrix effects of laser ablation of zircon and schorlomite are also investigated, and clearly demonstrate the necessity of a suitable matrix-matched reference material. The reliability and validity of our methodology is shown by analysis of five schorlomite samples encompassing an age range from 96 Ma to 1160 Ma as determined from other accessory minerals using K (Ar)–Ar, Rb–Sr, U–Pb, Lu–Hf, or fission track methods.

2. Experimental

All schorlomite samples investigated were analyzed for major and trace element contents together with U–Pb ages by electron microprobe and laser probe techniques (Appendix Tables 1S–3S†). All analyses were conducted at the State Key Laboratory of Lithospheric Evolution (SKLLE), the Institute of Geology and Geophysics, Chinese Academy of Sciences (IGG, CAS), Beijing.

2.1. Sample preparation

The schorlomites were separated by magnetic and electromagnetic means and concentrated with heavy liquids. They were then selected by hand using a binocular microscope until a purity >99% was attained. All separated crystals were embedded in one inch epoxy mounts and polished until the mineral grains were just revealed. Transmitted and, reflected light together with back-scattered electron (BSE) images (Fig. 1) were utilized to examine the internal features of the schorlomite such as inclusions, cracks and compositional zoning, and to provide a base map for recording laser spot locations. The grain mount was cleaned and left in 2% HNO_3 for several minutes prior to laser ablation analysis. The schorlomite crystals are black or brown-black in colour with a metallic or bituminous luster. Optically, the grains are opaque and isotropic, with thin edges of a brown-red colour. Compositional zoning was not observed either optically or by BSE-imagery. Major element compositions were obtained by using a JEOL-JAX8100 electron microprobe with 15 kV accelerating potential and 12 nA beam current. Counting times were 20 s. Total iron is expressed as Fe_2O_3. The analytical uncertainties are within 2% for TiO_2 and CaO, but ~10–20% for other minor elements due to their low concentrations (Appendix Table 1S†).

2.2. Schorlomite reference material

A well-characterized matrix-matched reference material is essential for U–Pb analytical techniques using ion or laser probes. Unfortunately, unlike other well-characterized mineral reference materials with a wide distribution (*e.g.*, zircon, monazite, apatite, titanite), there are no reference schorlomites available for laser ablation.

To remedy this deficiency we separated a schorlomite (WS20) from a wollaston ite-ijolite found at the Prairie Lake carbonatite complex, Northwestern Ontario, Canada,[8] for use as an in house primary reference material as the age of this complex is well-constrained by other geochronological methods. The Prairie Lake complex is composed of carbonatite, ijolite suite rocks and potassic nepheline syenite (malignite).[9] Two samples of baddeleyite from carbonatite yield SIMS U–Pb ages of 1157.2 ± 2.3 Ma and 1158.2 ± 3.8 Ma, identical to the ID-TIMS U–Pb age of 1163.6 ± 3.6 Ma obtained for baddeleyite from ijolite. Apatite

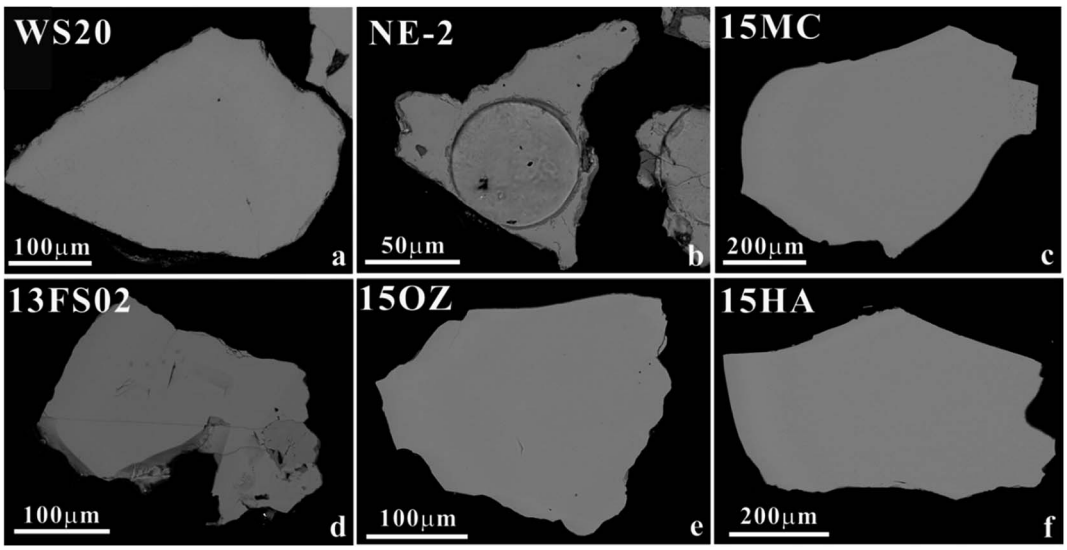

Fig. 1 Back-scattered electron (BSE) images of the homogeneous schorlomite samples investigated showing the absence of compositional zonation.

from the carbonatite yields the same U–Pb age of ~1160 Ma using ID-TIMS, SIMS and laser ablation techniques. These data indicate that the various rocks forming this complex were synchronously emplaced at about 1160 Ma.[8] Therefore, we assumed a Concordia age of ~1160 Ma for schorlomite (WS20) (Fig. 1a).

2.3. Instrumentation

Experiments were undertaken using an Agilent 7500a ICP-MS instrument (Agilent Technologies, Japan) coupled with an excimer 193 nm laser ablation system (Geolas 2005, Lambda Physic, Gottingen, Germany). The detailed description of instrumentation can be found elsewhere.[6] A spot size of 60 μm with a repetition rate of 8 Hz, the fluence of ~10 J cm^{-2}, was applied to our schorlomite measurements. The instrumental setup and operating conditions employing robust plasma conditions are reported in Table 1.

2.4. Mass spectrometry

The analytical protocol for U–Pb age determinations and trace elements abundances (including REE) are similar to those used for LA-ICP-MS U–Pb age determination of accessory minerals. A detail summary of the LA-ICP-MS specifications and typical operating conditions used in this study are summarized in Table 1. Helium was used as the carrier gas through the ablation cell and was merged with argon (make-up gas) downstream of the ablation cell. Prior to analysis, the pulse/analogy (P/A) factor of the detector was calibrated using standard tuning solution. The carrier and make-up gas flows were optimized to obtain maximal signal intensity for $^{238}U^{+}$, while keeping the ThO^{+}/Th^{+} ratio below 0.5% by laser sampling NIST SRM 612. All LA-ICP-MS measurements were carried out using time-resolved analysis in, peak-jumping mode. Each spot analysis consists of an approximately 25 s background acquisition and 65 s sample data acquisition. During routine analysis, background intensities were measured on-peak with laser off for the initial 25 s, and then, the laser was fired onto the samples for 65 s. The dwell time for each isotope was set at 6 ms for Si, Ca, Ti, Rb, Sr, Ba, Nb, Ta, Zr, Hf and REE, 10 ms for ^{232}Th, ^{238}U, 15 ms for ^{204}Pb, ^{206}Pb, ^{208}Pb, and 30 ms for ^{207}Pb (Table 1). The in house matrix-matched external reference schorlomite (WS20) was used to correct for U–Pb fractionation and instrumental mass discrimination. Two WS20 analyses were measured after every five schorlomite sample spots.

Table 1 Instrumental setup and operating conditions

ICP-MS Instrument	
Make, model and type	Agilent 7500a ICP-Q-MS
RF power (W)	1400 W
Cooling gas (L min^{-1})	16 L min^{-1}
Auxiliary gas (L min^{-1})	0.95 L min^{-1}
Sample gas (L min^{-1})	0.75–0.85 L min^{-1}
Torch H (mm)	1.1 mm
Torch V (mm)	−0.6 mm
Sampling depth (mm)	3.0 mm
Sample cone (mm)	1.0 mm
Skimmer cone (mm)	0.4 mm
Ion optics extraction 1 (V)	−200 V
Ion optics extraction 2 (V)	−120 V
Detector mode	Dual (cross-calibrated pulse/analogy modes)
Sensitivity	200 Mcps per ppm on ^{89}Y signal *via* 100 μL min^{-1} PFA nebulizer
Integration time (ms)	15 ms for ^{204}Pb, ^{206}Pb & ^{208}Pb, 30 ms for ^{207}Pb, 10 ms for ^{232}Th & ^{238}U, 6 ms for other elements
Dwell time (ns)	15 ns
Laser ablation system	
Make (model and type)	Geolas (complex 102; Lambda Physics)
Ablation cell	Standard circle cell from Geolas
Laser wavelength (nm)	193 nm ArF excimer laser
Pulse width (ns)	15 ns
Fluence (J cm^{-2})	~10 J cm^{-2}
Repetition rate (Hz)	8 Hz
Ablation duration (s)	65 s
Spot diameter (μm)	60 μm
Sampling mode/pattern	Static spot ablation
Cell carrier gas flow (L min^{-1})	~0.80 L min^{-1}

2.5. Data reduction

Trace element concentrations including U, Th, Pb and REE were calibrated against the NIST SRM 612 standard glass reference material using ^{43}Ca as an internal standard element using GLITTER laser ablation software (element concentrations) from Macquaire University.[11] For schorlomite quantification, CaO contents determined by electron microprobe were used (Appendix Table 1S†). All count rates each analysis were firstly normalized to the ^{43}Ca count rate, and then a time-drift correction was applied by using a linear interpolation with time for every ten analysis using the variation of signal intensity ratios of NIST SRM 612.

For schorlomite signals of the ^{204}Pb, ^{206}Pb, ^{207}Pb, ^{208}Pb, ^{232}Th and ^{238}U masses were acquired for U–Pb age determination, with the ^{235}U signal calculated from ^{238}U on the basis of the $^{238}U/^{235}U$ ratio of 137.88. The GLITTER software (isotope ratio)[11] was used to calculate U–Pb data from the raw signals. Isotopic ratios were calculated from the background subtracted signal for the corresponding isotopes. Corrections for instrumental mass bias, ablation-related fractionation and instrumental drift were performed simultaneously, employing a standard-sample-standard bracketing method. Taking in account the negligible common Pb content (Fig. 2a) of WS20 schorlomite, in addition to the uniform U, Th, Pb and REE contents, the preferred U–Th–Pb isotopic ratios used for our WS20 schorlomite reference material were obtained from the assumption of a 1160 Ma concdia age.[8] All the measured $^{207}Pb/^{206}Pb$, $^{207}Pb/^{235}U$ and $^{206}Pb/^{238}U$ isotopic ratios of the schorlomite during the process of sample analyses were linearly regressed and corrected using WS20 as the primary reference value for the U–Pb age (Fig. 2a). Standard deviations of the calibrated isotope ratios include those from sample, external

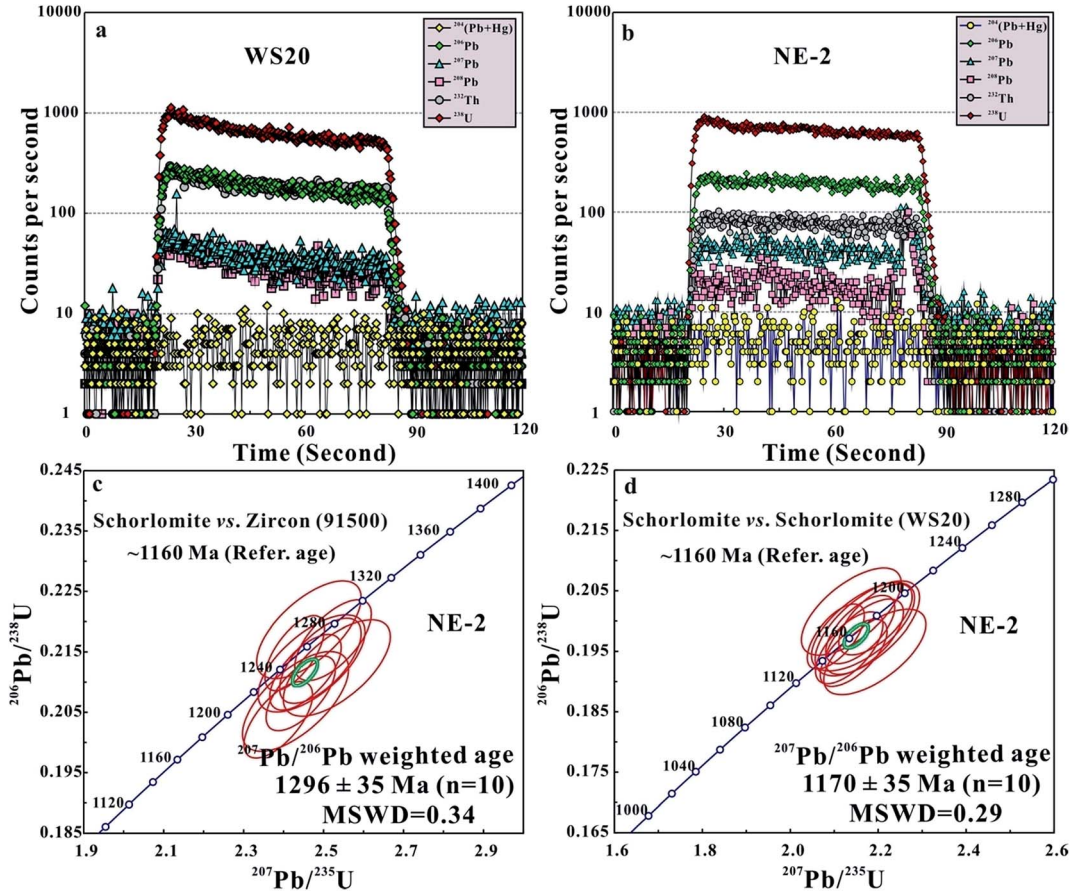

Fig. 2 (a & b) Illustrate time *vs.* signal sensitivity evolving of laser ablating schorlomite (WS20 & NE-2) for a typical measurement, indicating that WS20 or NE-2 schorlomite has negligible or very low common Pb. (c & d) Demonstrate that matrix effects of schorlomite and zircon investigated during laser ablation for U–Pb age determination of schorlomite NE-2. The results show that there is significant matrix effect for both of these minerals. (c) Shows the concordant U–Pb age and weighted mean ^{207}Pb/^{206}U age of the schorlomite (NE-2) sample using the zircon standard (91 500) for external calibration, whereas (d) shows data for schorlomite (NE-2) using the in house schorlomite standard (WS20) as the external calibration during the same analytical session (see text for discussion). Abbreviation: MSWD, Mean Square of Weighted Deviates.

standard, and deviations from the reference values of the external standard. The uncertainty of the schorlomite standard reference was set at 2%. The U–Pb concordia ages and ^{206}Pb/^{238}U weighted mean ages or Tera–Wasserburg diagrams, intercepted age without any common Pb correction, were calculated or illustrated with the ISOPLOT/EX 3.23 software package.[10]

2.6. Matrix effects for zircon and schorlomite

To evaluate matrix effects, we initially investigated these using zircon (91 500) or schorlomite (WS20) as the external calibration standard during the same analytical session (Fig. 2a and b). As shown in Fig. 2c, our obtained ^{207}Pb/^{206}Pb weighted age (1296 ± 35 Ma) of NE-2 schorlomite from the Prairie Lake carbonatite complex using the zircon (91 500) is 11% older than the reference value (1160 Ma). However, our obtained ^{207}Pb/^{206}Pb weighted age (1170 ± 35 Ma) of NE-2 agrees well with the recommended value using the WS20 schorlomite (Fig. 2d).[8] These data demonstrate clearly that there are significant matrix effects between schorlomite and zircon during laser ablation, indicating that suitable matrix-matched standard is essential for U–Pb geochronology of schorlomite using LA-ICP-MS (Fig. 2c and d). In all of the U–Pb data presented below WS20 was used as the primary schorlomite reference material (Fig. 2a).

3. Result and discussion

In order to validate and demonstrate the effectiveness and robustness of our protocol, we undertook U–Pb age determinations of several separate schorlomite samples from four typical alkaline complexes. Representative major and trace element compositions of these schorlomites are given in the appendix (Tables 1S and 2S†), and the individual REE distribution patterns for these schorlomites are presented in Fig. 3. Fig. 4 & 5 show the illustration of time *vs.* signal intensity for typical analytical runs during laser ablation of schorlomite and the concordant U–Pb ages, weighted mean ^{206}Pb/^{238}U ages and Tera–Wasserburg diagrams intercept ages as determined in this study with the U–Pb isotopic data given in Appendix (Table 3S†).

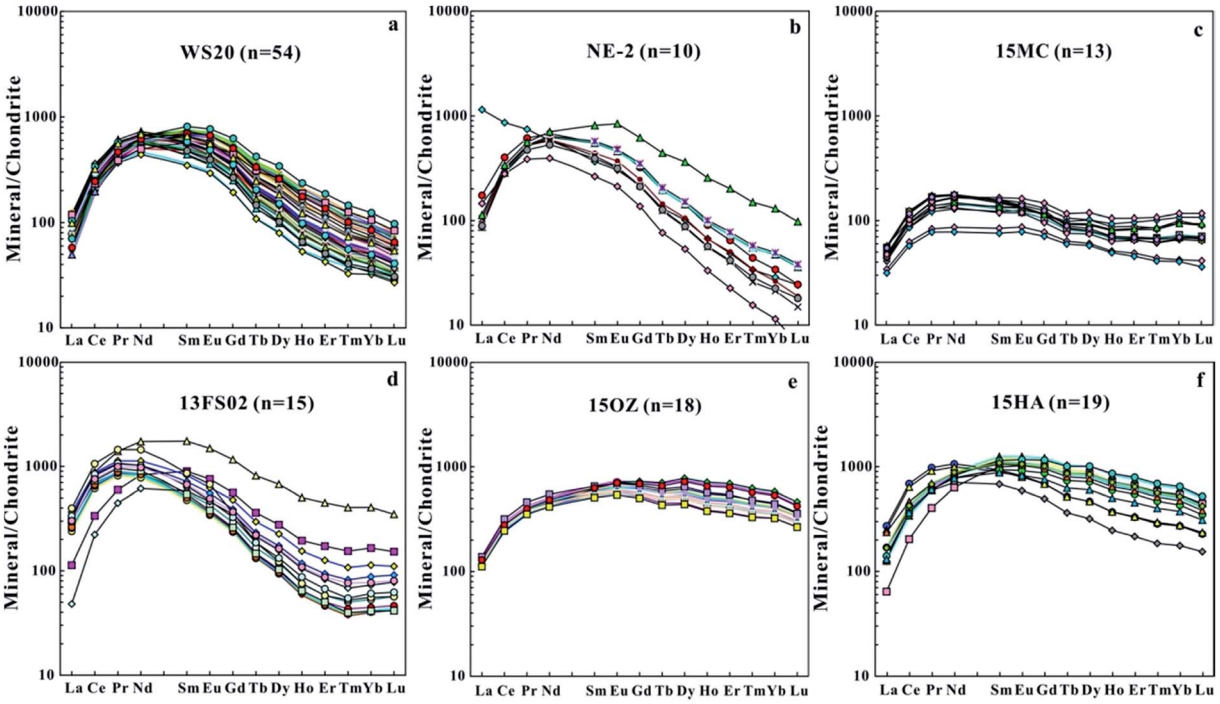

Fig. 3 The chondrite-normalized REE distribution patterns of individual schorlomites from: Magnet Cove (15MC); Arkansas (USA); Fanshan ultrapotassic complex (13FS02), Hebei (China); Ozernaya (15OZ) alkaline ultramafic complex, Kola Peninsula (Russia); Alnö (15HA) alkaline carbonatite complex (Sweden); and the Prairie Lake carbonatite complex (WS20 and NE-2), Northwestern Ontario, Canada.

3.1. Results

Sample 15MC, is from the Magnet Cove Complex, Hot Springs County, Arkansas (USA) (Fig. 1c). The geology of this complex has been described by Erickson & Blade.[12] As shown in Fig. 5a, our thirteen analyses of this schorlomite yielded a concordant weighted mean $^{206}Pb/^{238}U$ age of 96.4 ± 1.8 Ma (MSWD = 0.53) (Fig. 4a). Zartman *et al.*[13] previously obtained K–Ar biotite ages of 97 ± 5 Ma and 95 ± 5 Ma from alkali syenite, and also determined a Rb–Sr age of 99 ± 8 Ma for the garnet ijolite. Naeser and Faul[14] obtained a fission track apatite age of 97 ± 10 Ma from a carbonatite and a fission track titanite age of 102 ± 10 Ma from a nepheline syenite. Eby[15] reported an average fission track titanite age for the complex of 101.4 ± 1.0 Ma, fission track apatite ages determined for all of the intrusive units are between 95.9 and 101.4 Ma. Thus, our laser-acquired U–Pb age is in excellent agreement with data obtained using K–Ar, Rb–Sr, or fission track methods,[16] and demonstrates the better precision and accuracy over other methods of geochronology.

Sample 13FS02 is from the Fanshan ultrapotassic complex, Hebei (China) (Fig. 1d). Further details of the schorlomite paragenesis and the geology of this alkaline complex are provided by Wu & Mu,[17] and Hou *et al.*[18] Our fifteen analyses yielded a intercepted age of 229.9 ± 3.7 Ma (MSWD = 0.65) in Tera–Wasserburg diagrams (Fig. 4b and 5b). Niu *et al.*[19] previously reported a zircon U–Pb age of 224.9 ± 3.1 Ma using LA-ICP-MS. Recently, Li *et al.*[20] undertook two Lu–Hf age determinations of separated apatite, biotite and clinopyroxene from this complex and obtained apatite Lu–Hf ages of 226.5 ± 3.6 Ma (10FW04) and 231.3 ± 3.1 Ma (10FW09), respectively. Two baddeleyites SIMS U–Pb age determinations of the complex by Li *et al.*[20] yielded emplacement ages of 227.0 ± 3.5 Ma (13FS01) and 220.5 ± 2.9 Ma (13FS03), respectively. These data indicate that various minerals, including schorlomite, are coeval within a narrow age range.

Sample 15OZ is from the Ozernaya alkaline ultramafic complex, Kola Peninsula (Russia) (Fig. 1e). Further details on the paragenesis of the schorlomite and the geology of the complex are provided by Wu *et al.*[21] and Arzamastsev & Wu.[22] Our eighteen analyses yield a concordant weighted mean $^{206}Pb/^{238}U$ age of 386.1 ± 4.7 Ma (MSWD = 0.53) (Fig. 4c and 5c). Wu *et al.*[21] obtained an ID-TIMS U–Pb age of 386.1 ± 1.4 Ma (n = 4) for perovskite from this complex. Arzamastsev & Wu[22] reported ^{207}Pb corrected $^{206}Pb/^{238}U$ perovskite ages of 383 ± 6 Ma (n = 18) and 374 ± 5 Ma (n = 18) using LA-ICP-MS. These data indicate coeval perovskite and schorlomite emplacement ages for this complex.

Sample 15HA is from the Alnö alkaline carbonatite complex (Sweden) (Fig. 1f). The geology of this complex has been described by von Eckermann.[23] Our nineteen analyses yielded a intercepted age of 587.5 ± 7.4 Ma (MSWD = 0.059) in Tera–Wasserburg diagrams (Fig. 4d and 5d). Andersen[24] obtained a whole rock Pb–Pb isochron age of 584 ± 13 Ma as the best estimate of the crystallization age of the complex. Meert *et al.*[25] reported a 584 ± 7 Ma age using $^{40}Ar/^{39}Ar$ age determinations of biotite and K-feldspar. Rukhlov & Bell[26] reported 589.7 ± 4.4 Ma (P2-036) and 582.8 ± 5.7 Ma (P2-037) ages using ID-TMS methods for baddeleyite and apatite, respectively. Thus, our

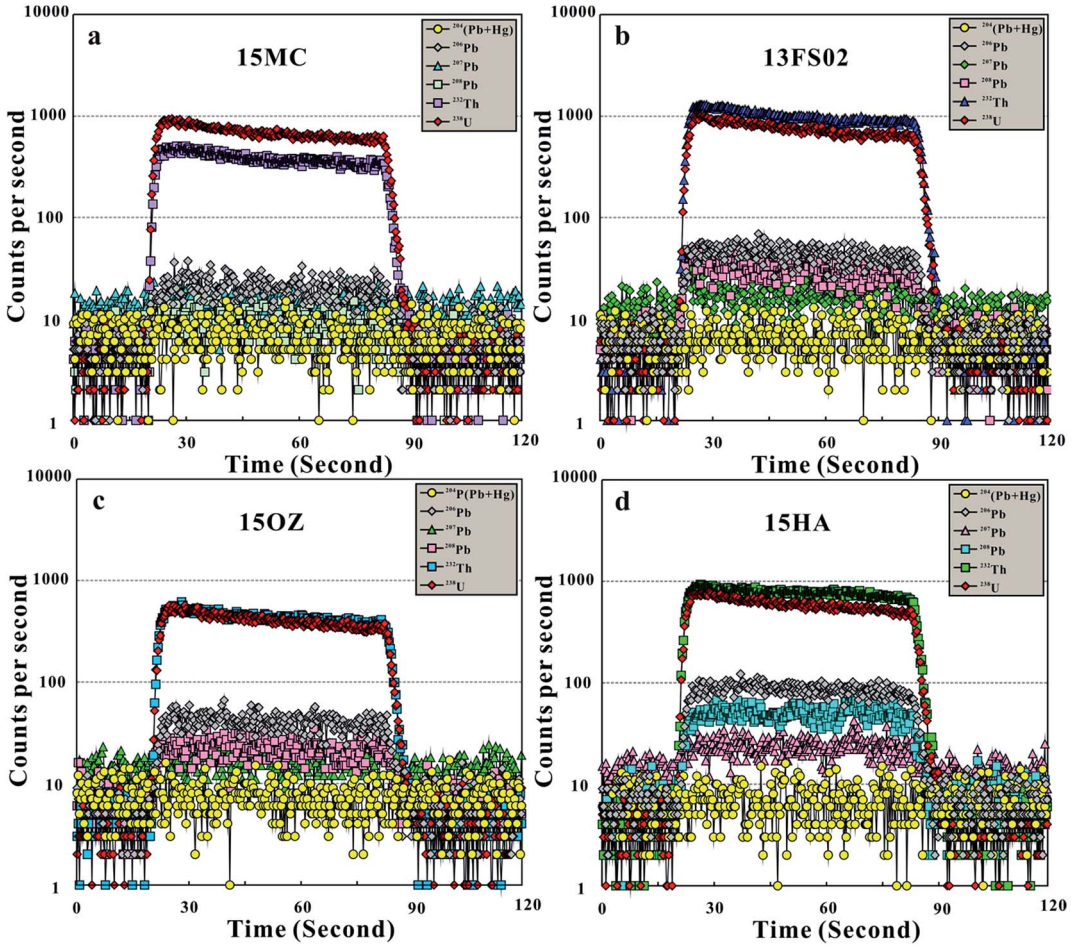

Fig. 4 A plot of time *vs.* signal sensitivity evolving for a typical analysis during laser ablating schorlomites (15MC, 13FS02, 15OZ & 15HA). It indicates schorlomite investigated in this work has negligible or very low common Pb (see text for discussion).

schorlomite U–Pb age agrees well with those obtained previously by various methods.

3.2. U–Pb age measurement of schorlomite

As shown in Fig. 6, schorlomites exhibit a relatively narrow range of U contents (10–40 ppm), whereas Th contents exhibit a wider range of 2–90 ppm. Therefore, it is possible to determine precisely the U–Pb isotopic composition, by either ID-TIMS or *in situ* techniques (LA-(MC)-ICP-MS or SIMS). Moreover, U–Pb geochronology is preferable to Th–Pb methods considering the relatively lower Th/U ratios of schorlomite (Table 2S,† Fig. 6). Fortunately, the five schorlomites, investigated in this work gave consistent U–Pb ages with concordia or lower common Pb contents. This is a significant observation with respect to the potential of schorlomite for U–Pb geochronology.[5,6]

No common Pb correction has been applied during data processing. Of the six schorlomite samples evaluated for geochronology in this study, four (WS20, NE-2, 15MC, 15OZ) gave concordant results and two (13FS02, 15HA) gave discordant results. The influence of common Pb was evident in the two discordant samples, as illustrated by Terra–Wasserburg diagrams (Fig. 4 and 5). This is probably due to common Pb-rich inclusions within the schorlomite grains.

3.3. Schorlomite closure temperatures

The closure temperature of schorlomite with respect to the U–Pb system has not been evaluated previously. Petrographic observations have indicated that the mineral is susceptible to alteration in the later stages of the evolution of alkaline magmas or by deuteric hydrothermal fluid activity.[8] Such alteration could disturb and reset the original U–Pb isotopic system. In order to understand fully the U–Pb closure temperature of schorlomite, a calculation of diffusion coefficients using the kinetic porosity model of Zhao and Zheng[27] is shown in Fig. 7. From these data it is apparent that schorlomite has a relatively slow Pb diffusion rate and higher closure temperatures for crystals of small radius (*ca.* <100 μm). However, there are almost similar closure temperatures for schorlomite and titanite for larger grains.

3.4. Potential *in situ* reference material for U–Pb age of schorlomite

For *in situ* analysis, a corresponding reference material is a prerequisite (*e.g.*, zircon, apatite, monazite, titanite).[6,8,28,29] To

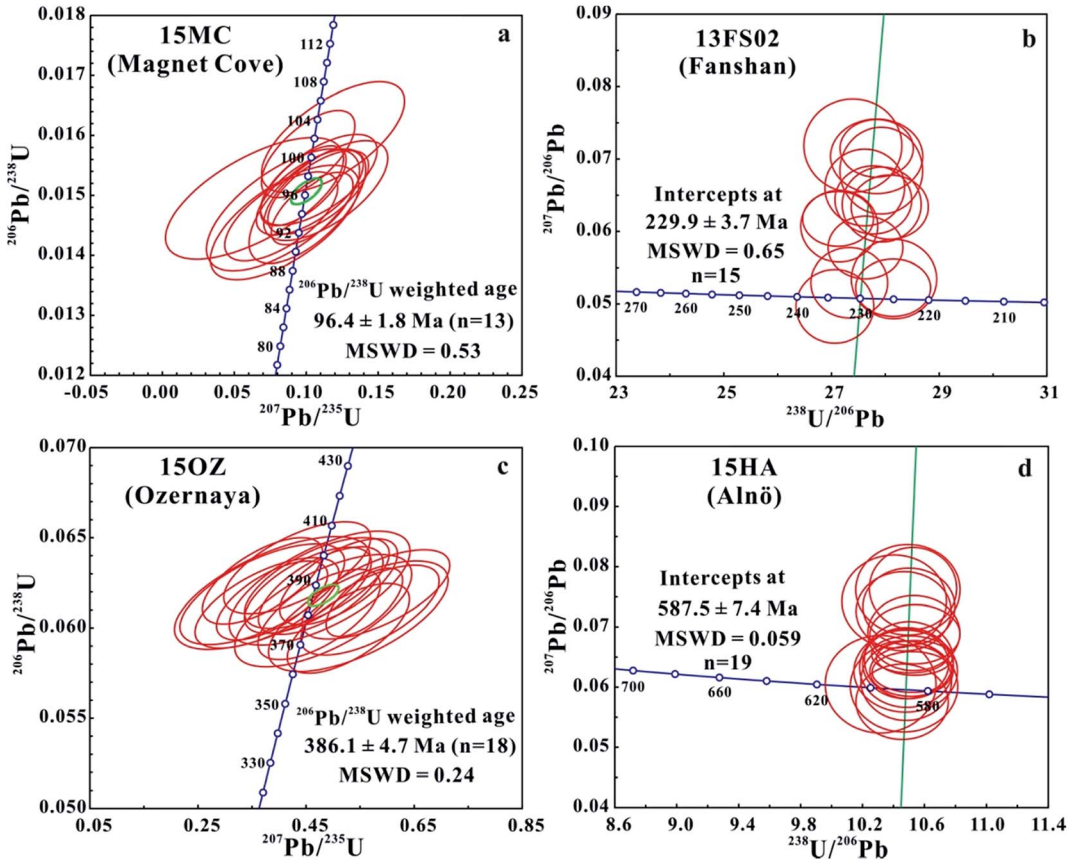

Fig. 5 The concordant U–Pb ages and weighted mean $^{206}Pb/^{238}U$ ages of schorlomites (15MC & 15OZ), Tera–Wasserburg plots and intercepts ages of schorlomites (13FS02 & 15HA). These data indicate that our U–Pb ages of schorlomite are consistent with age determinations of diverse minerals from these localities (see text for discussion). Abbreviation: MSWD, Mean Square of Weighted Deviates.

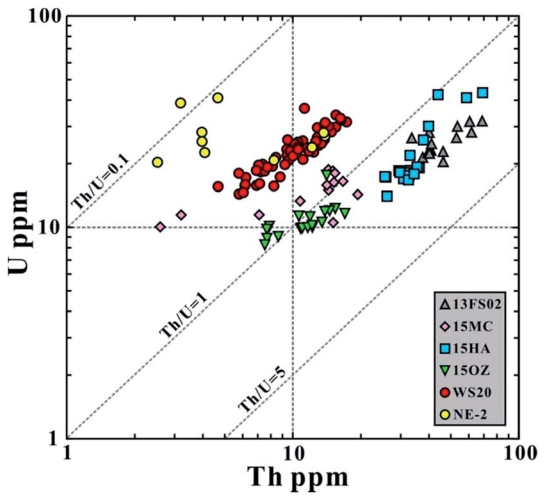

Fig. 6 Th and U concentration and Th/U ratio of schorlomite investigated in this study, indicating 10–50 ppm of U with a relatively narrow range and a relatively wider 2–90 ppm of Th content. Therefore, U–Pb age determination is considered to be preferable to Th–Pb methods with relatively lower Th/U ratios, considering concordant U–Pb age or lower common Pb content.

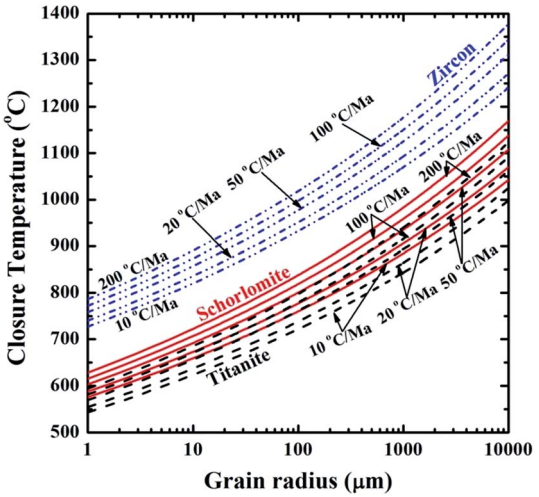

Fig. 7 Calculation of Pb closure temperatures in schorlomite, titanite and zircon based on the methods of Zhao and Zheng (2007).[27] Note that schorlomite has a Pb closure temperature of ~750–800 °C for grains with a size of 100 μm at cooling rates of 10–200 °C per Ma, indicating the Pb closure temperature of schorlomite is the similar to that of titanite (Wu *et al.*, 2010).[28,29]

date, there are no schorlomite reference materials except for our in house standard WS20 from the Prairie Lake carbonatite complex.

Candidate reference materials for matrix-matched U–Pb age determination should have following requirements: (a) the trace element concentration should be homogenous both within and between individual grains; (b) they should exhibit high U contents with as low a common Pb content as possible; (c) a knowledge of the crystallization age (*e.g.* U–Pb ages) is required for isotopic analyses so the initial isotopic composition can be calculated; (d) they should be readily available, ideally as large crystals in sufficient quantity to supply the scientific community.

On the above basis, the 15MC and 15OZ schorlomites with homogenous U contents (~10 ppm U) yielded concordant U–Pb age and are ideal secondary *in situ* U–Pb reference materials although of relatively younger U–Pb ages (Fig. 6). Considering their more radiogenic Pb, the relatively older WS20 and 15HA samples with moderate U content make them suitable primary reference materials for schorlomite U–Pb geochronology (Fig. 5 and 6). To investigate further schorlomite U–Pb geochronology, additional numerous and precise ID-TIMS U–Pb age determinations are necessary to consider them as well-characterized reference material, although the LA-ICP-MS data presented here are self-consistent. More precise ID-TIMS U–Pb ages of schorlomite are required to improve the accuracy of the fractionation correction and age determinations of unknown using *in situ* techniques in our future work.[29,30]

4. Conclusions

In this work, we demonstrate for the first time that it is possible to use schorlomite garnet for U–Pb geochronology using LA-ICP-MS. The matrix effects between zircon and schorlomite are also investigated and compared in detail during laser ablation, and indicate the necessity of using a suitable matrix-matched reference material. Laser-induced elemental fractionation and instrumental mass discrimination were externally corrected using our in house reference schorlomite material (WS20; 1160 Ma U–Pb age). In order to validate and demonstrate the effectiveness and robustness of our analytical protocol, we applied our methods for the U–Pb age determination of five typical schorlomite samples from alkaline rock–carbonatite complexes, and show that schorlomite U–Pb ages agree well with radiometric ages previously obtained by diverse methods. Because of its relatively high U and Th contents and common occurrence in carbonatite and alkaline rocks, schorlomite is an ideal mineral for U–Pb isotopic age determinations. Our novel conclusions are that is not only possible to obtain realistic U–Pb age determinations of schorlomite but also the observation that this mineral because of the low common Pb contents gives reliable U–Pb Concordia ages. Thus, the LA-ICP-MS U–Pb age determination of schorlomite can be considered as a promising geochronological method applicable to carbonatites, alkaline rocks, and related rare-metal deposits.

Conflicts of interest

There are no conflicts to declare.

Acknowledgements

This work was financially supported by the Natural Science Foundation of China (NSFC Grants 41525012, 41473012 and 41403002), National Key R&D Program of China (2017YFC0601306) and Excellent Collective Laboratory of Beijing Regional Center of Earth Systems & Environment Science Instrument by the Chinese Academy of Sciences (Y722801228). Two anonymous reviewers are also grateful for critical and insightful comments that significantly improved this manuscript. We are also indebted to those schorlomite sample providers (*e.g.*, Gunnar Färber Mineralien (15MC, 15HA)). We are particularly thankful to Prof. Qiu-Li Li, Prof. Chao-Feng, Li and Prof. Zhu-Yin Chu for their fruitful discussions and suggestions and Dr Neng Jiang and Yang Li for their help during sample preparation and mass spectrometric measurement. We also thank the editor for his patience while handling our manuscript.

References

1 E. S. Grew, A. J. Locock, S. J. Mills, I. O. Galuskina, E. V. Galuskin and U. Hålenius, *Am. Mineral.*, 2013, **98**, 785–811.
2 S. Duchene, J. Blichert-Toft, B. Luais, P. Telouk, J. Lardeaux and F. Albarede, *Nature*, 1997, **387**, 586–588.
3 J. Harvey and E. F. Baxter, *Chem. Geol.*, 2009, **258**, 251–257.
4 S. Seman, D. F. Stockli and N. M. McLean, *Chem. Geol.*, 2017, **460**, 106–116.
5 X. D. Deng, J. W. Li, T. Luo and H. Q. Wang, *Contrib. Mineral. Petrol.*, 2017, **172**, 71–81.
6 Y. H. Yang, F. Y. Wu, Y. Li, J. H. Yang, L. W. Xie, Y. Liu, Y. B. Zhang and C. Huang, *J. Anal. At. Spectrom.*, 2014, **29**, 1017–1023.
7 R. E. Ernst and K. Bell, *Mineral. Petrol.*, 2010, **98**, 55–76.
8 F. Y. Wu, R. H. Mitchell, Q. L. Li, C. Zhang and Y. H. Yang, *Geol. Mag.*, 2017, **154**, 217–236.
9 S. E. Zurevinski and R. H. Mitchell, *Lithos*, 2015, **239**, 234–244.
10 K. R. Ludwig, *Isoplot*, 2003, **3**, 1–70.
11 W. L. Griffin, W. J. Powell, N. J. Pearson and S. Y. O'Reilly, in *Laser ablation ICP-MS in the Earth sciences: current practices and outstanding issues*, ed. P. Sylvester, Mineralogical Association of Canada. Short course series, Quebec, 2008, vol. 40, pp. 308–311.
12 R. L. Erickson, and L. V. Blade, 1963, *U. S. Geol. Soc. Profess. Paper*, vol. 425, p. 94.
13 R. E. Zartman, M. R. Brock, A. V. Hey and H. H. Thomas, *Am. J. Sci.*, 1967, **265**, 848–870.
14 C. W. Naeser and H. Faul, *J. Geophys. Res.*, 1969, **74**, 705–710.
15 G. N. Eby, *U. S. Geol. Survey Open File Report*, 1987, pp. 87–0287.

16 B. R. Globerman and E. Irving, *J. Geophys. Res.*, 1988, **93**, 721–733.
17 G. B. Wu and B. L. Mu, *Phys. Chem. Miner.*, 1986, **13**, 198–205.
18 T. Hou, Z. C. Zhang, J. K. Keiding and I. V. Veksler, *J. Petrol.*, 2015, **56**, 893–918.
19 X. L. Niu, B. Chen, A. K. Liu, K. Suzuki and X. Ma, *Lithos*, 2012, **149**, 146–158.
20 Y. Li, *CAS. P60 (In Chinese with English abstract)*, The University of Chinese Academy of Sciences and Institute of Geology and Geophysics, 2016.
21 F. Y. Wu, A. A. Arzamastsev, R. H. Mitchell, Q. L. Li, J. Sun, Y. H. Yang and R. C. Wang, *Chem. Geol.*, 2013, **353**, 210–229.
22 A. A. Arzamastsev and F. Y. Wu, *Petrology*, 2014, **22**, 462–479.
23 H. Eckermann (von), *The alkaline district of Alno isoland*, Geological Survey of Sweden (SGU), 1948, vol. 38, p. 176.
24 T. Andersen, *Abstract volume. 22nd Nordic Geological Winter Meeting*, 1996, p. 11.
25 J. G. Meert, H. J. Walderhaug, T. H. Torsvik and B. W. H. Hendriks, *Precambrian Res.*, 2007, **154**, 159–174.
26 A. S. Rukhlov and K. Bell, *Mineral. Petrol.*, 2010, **98**, 11–54.
27 Z. F. Zhao and Y. F. Zheng, *Am. Mineral.*, 2007, **92**, 289–308.
28 F. Y. Wu, Y. H. Yang, M. A. W. Marks, Z. C. Liu, Q. Zhou, W. C. Ge, J. S. Yang, Z. F. Zhao, R. H. Mitchell and G. Markl, *Chem. Geol.*, 2010, **273**, 8–34.
29 L. W. Xie, J. H. Yang, Q. Z. Yin, Y. H. Yang, J. B. Liu and C. Huang, *J. Anal. At. Spectrom.*, 2017, **32**, 975–986.
30 Y. H. Yang, H. F. Zhang, Z. Y. Chu, L. W. Xie and F. Y. Wu, *Int. J. Mass Spectrom.*, 2010, **290**, 120–126.